Three-Dimensional Structure of the Binuclear Metal Center of Phosphotriesterase†

Matthew M. Benning,*,‡ Jane M. Kuo,§ Frank M. Raushel,§ and Hazel M. Holden*,‡

Institute for Enzyme Research, Graduate School and Department of Biochemistry, University of Wisconsin, Madison, Wisconsin 53705, and Department of Chemistry, Texas A&M University, College Station, Texas 77843

Received March 23, 1995; Revised Manuscript Received April 25, 1995®

ABSTRACT: Phosphotriesterase, as isolated from *Pseudomonas diminuta*, is capable of detoxifying widely used pesticides such as paraoxon and parathion and various mammalian acetylcholinesterase inhibitors. The enzyme requires a binuclear metal center for activity. Recently, the three-dimensional structure of the apoenzyme was solved (Benning *et al.*, 1994) and shown to consist of an α/β-barrel. Here we describe the three-dimensional structure of the holoenzyme, reconstituted with cadmium, as determined by X-ray crystallographic analysis to 2.0-Å resolution. Crystals employed in the investigation belonged to the space group $C2$ with unit cell dimensions of $a = 129.5$ Å, $b = 91.4$ Å, $c = 69.4$ Å, $\beta = 91.9°$, and two subunits in the asymmetric unit. There are significant differences in the three-dimensional architecture of the apo and holo forms of the enzyme such that their α-carbon positions superimpose with a root-mean-square deviation of 3.4 Å. The binuclear metal center is located at the C-terminus of the β-barrel with the cadmiums separated by 3.8 Å. There are two bridging ligands to the metals: a water molecule (or possibly a hydroxide ion) and a carbamylated lysine residue (Lys 169). The more buried cadmium is surrounded by His 55, His 57, Lys 169, Asp 301, and the bridging water in a trigonal bipyramidal arrangement. The second metal is coordinated in a distorted octahedral geometry by His 201, His 230, Lys 169, the bridging water molecule, and two additional solvents.

The phosphotriesterase isolated from *Pseudomonas diminuta* and *Flavobacterium* sp. catalyzes the detoxification of organophosphate nerve agents with a surprisingly high turnover. The k_{cat} values for the best substrates, such as paraoxon, for example, approach nearly 10^4 s^{-1} at 25 °C (Omburo *et al.*, 1992). In spite of the fact that phosphotriesters (and the related phosphonates) are not natural products, the bacterial enzyme apparently has evolved, within a relatively short time frame, to specifically hydrolyze this functional group. Recently Scanlan and Reid (1995) have shown that the nucleic acid sequence of the *Escherichia coli* chromosomal region from 67.4 to 76.0 min encodes a protein with significant amino acid sequence homology to phosphotriesterase. They have termed this protein "phosphotriesterase homology protein" (PHP). Phosphotriesterase and PHP display a 28% identity and a 66% similarity over most of their primary structure leading Scanlan and Reid to propose that PHP is part of the family from which the phosphotriesterase may have evolved.

The precise mechanism for the chemical transformation catalyzed by phosphotriesterase is not known in great detail. It has been demonstrated, however, that the product of the reaction is formed with a net inversion of stereochemistry at the phosphorus center (Lewis *et al.*, 1988). This result argues against a phosphorylated enzyme intermediate and strongly suggests that the reaction is facilitated by an activated water molecule (or hydroxide) that directly attacks the substrate in a single chemical step. The most salient feature of the active site has been shown thus far to be a binuclear metal center of unknown structure that presumably functions to activate the hydrolytic water molecule and perhaps the substrate for the subsequent nucleophilic attack and expulsion of the leaving group. As naturally isolated, the enzyme contains up to 2 equiv of zinc per subunit.

The structure of the binuclear metal center has not been described thus far but Zn^{2+}, Cd^{2+}, Ni^{2+}, Co^{2+}, and Mn^{2+} are all catalytically active (Omburo *et al.*, 1992). EPR spectra of the Mn^{2+}/Mn^{2+}-substituted enzyme have shown that the two metal ions within this center are antiferromagnetically coupled through a common ligand (Chae *et al.*, 1993). NMR spectra of the ^{113}Cd-substituted enzyme have indicated that the first coordination shell for each metal is composed of a mixture of oxygen and nitrogen ligands with the exclusion of any thiolate from cysteine residues (Omburo *et al.*, 1993).

The relative importance of histidine residues in metal ligation was confirmed by site-specific mutation of all seven histidine residues in the protein. The mutagenesis investigations predicted that six of the seven histidine residues were at or near the active site and contributed to the structure and/or catalytic function of the enzyme (Kuo & Raushel, 1994; Lai *et al.*, 1994). These studies were confirmed with the recent solution of the three-dimensional structure of the apoenzyme by X-ray crystallographic analyses (Benning *et al.*, 1994). As observed in various other enzymes, the molecular fold of phosphotriesterase is a simple α/β-barrel with eight strands of parallel β-pleated sheet. Although this first crystal structure was determined without bound metal ions, the predicted cluster of six histidine residues was found at the C-terminus of the β-barrel where the active sites for enzymes containing this structural motif are invariably located. The X-ray crystallographic investigation of the apoenzyme also demonstrated its quaternary structure to be dimeric rather than monomeric as originally proposed. Each

† This research was supported in part by grants from the NIH (GM-33894 to F.M.R. and DK-47814 to H.M.H.).

* To whom correspondence should be addressed.

‡ University of Wisconsin.

§ Texas A&M University.

® Abstract published in *Advance ACS Abstracts,* May 15, 1995.

0006-2960/95/0434-7973$09.00/0

Table 1: Intensity Statistics

	resolution range (Å)							
	overall	100.00−4.00	3.17	2.77	2.52	2.34	2.20	2.09
no. of measurements	151079	30002	29773	25289	19391	14655	13251	10679
no. of independent reflections	49624	6846	6787	6719	6580	6352	6066	5550
completeness of data (%)	91	98	99	98	97	94	90	82
av intensity	4080	10000	6136	2683	1524	1085	816	585
av σ	233	361	298	216	175	150	144	138
R factor[a] (%)	4.0	3.2	3.8	5.2	6.4	7.0	8.3	10.0

[a] R factor = $(\Sigma|I - \bar{I}|/\Sigma I) \times 100$.

subunit of phosphotriesterase contains 336 amino acid residues.

Here we describe the three-dimensional structure of the holoenzyme containing 2 mol equiv of Cd^{2+}. The geometry around the more buried metal ion is trigonal bipyramidal with two nitrogen- and three oxygen-containing ligands. The second Cd^{2+} is ligated by two nitrogen- and four oxygen-containing ligands in a distorted octahedral arrangement. One of the bridging ligands is a carbamate formed from the reaction of CO_2 with the ϵ-amino group of Lys 169. A water molecule serves as the second bridging ligand. X-ray coordinates for the phosphotriesterase have been deposited in the Brookhaven Protein Data Bank (Bernstein *et al.*, 1977).

MATERIALS AND METHODS

Crystallization and X-ray Data Collection. The enzyme employed for crystallization trials was purified and reconstituted with Cd^{2+} according to published procedures, dialyzed against 10 mM HEPES, pH 8.5, and concentrated to 11 mg/mL (Omburo *et al.*, 1992).

Single crystals were grown by the hanging drop method of vapor diffusion at 4 °C. The precipitant contained 10% poly(ethylene glycol) 8000, 5 mM NaN_3, and 1% diethyl 4-methylbenzylphosphonate buffered with 50 mM CHES at pH 9.0. The crystals belonged to the space group $C2$, with unit cell dimensions of $a = 129.5$ Å, $b = 91.4$ Å, $c = 69.4$ Å, $\beta = 91.9°$, and two subunits in the asymmetric unit. They achieved maximum dimensions of 0.5 mm × 0.5 mm × 0.1 mm in approximately 1 week.

For X-ray diffraction experiments, the crystals were mounted in quartz capillary tubes and cooled to 4 °C. A native X-ray data set was collected to 2.0-Å resolution from a single crystal with a Siemens X1000D area detector system. The X-ray source was nickel-filtered Cu Kα radiation from a Rigaku RU200 X-ray generator operated at 50 kV and 50 mA and equipped with a 200-μm focal cup. A crystal-to-detector distance of 12 cm was used together with a step size of 0.15° per frame.

The X-ray data were processed with the data reduction software package XDS (Kabsch, 1988a,b) and internally scaled according to a procedure developed in the laboratory by Dr. Gary Wesenberg. Relevant X-ray data collection statistics may be found in Table 1. The X-ray data set was 91% complete to 2.0-Å resolution.

Molecular Replacement and Least-Squares Refinement. The structure of the holoenzyme was solved by the technique of molecular replacement with the software package AMORE (Navaza, 1987). The three-dimensional structure of the apoenzyme monomer served as the search model. The rotational and translational searches were conducted with X-ray data between the resolution range of 8−3.5 Å. Two solutions corresponding to the two molecules in the asymmetric unit were obtained as follows: (1) $\alpha = 317.9°$, $\beta = 78.7°$, $\gamma = 130.8°$, $a = 0.3405$, $b = -0.0002$, $c = 0.4036$ and (2) $\alpha = 42.6°$, $\beta = 98.8°$, $\gamma = 307.8°$, $a = 0.3434$, $b = 0.6186$, $c = 0.1089$. Following rigid body refinement, the R-factor was 45% for all X-ray data between 30 and 2.0 Å.

Table 2: Refinement Statistics

resolution limits (Å)	30.0−2.0
final R factor[a] (%)	15.2
no. of reflections used	49624
no. of atoms	5483
weighted root-mean-square deviations from ideality	
bond length (Å)	0.016
bond angle (deg)	2.351
planarity (trigonal) (Å)	0.007
planarity (other planes) (Å)	0.013
torsion angle[b] (deg)	16.122

[a] R factor = $\Sigma|F_o - F_c|/\Sigma|F_o|$. [b] The torsion angles were not restrained during refinement.

On the basis of the above solution, an electron density map was calculated to 2.0-Å resolution. Upon initial inspection of this map it became clear that there were several significant regions where the polypeptide chain, based on the apoenzyme model, did not follow the electron density. To expedite the rebuilding and least-squares refinement processes, these regions were removed from the model, and the electron density for the two molecules in the asymmetric unit was averaged according to the algorithm of Bricogne (1976). The model for the holoenzyme was subsequently rebuilt from this "averaged" map, placed back into the unit cell, and refined with the program TNT (Tronrud *et al.*, 1987).

Quality of the Model. Alternate cycles of least-squares refinement and manual model building at 2.0-Å resolution reduced the R factor to 15.2%. The Cd^{2+} and nitrogen or oxygen ligand distances were restrained to 1.8 Å. The Cd^{2+}/Cd^{2+} distance was restrained to 3.3 Å. Relevant refinement statistics may be found in Table 2, and a Ramachandran plot of all non-glycinyl residues is displayed in Figure 1. Small peaks of electron density within 3.5 Å of potential hydrogen-bonding groups were modeled as waters. A total of 420 solvent molecules was included in the refinement. Note that there were 659 observed amino acid residues in the asymmetric unit. The average temperature factors for all backbone atoms in subunits I and II were 20.8 and 19.7 Å^2, respectively.

A representative portion of the electron density map is shown in Figure 2. For the most part the electron density was very well ordered except for the following surface residues: Arg 67, Lys 77, Arg 96, Lys 175, Arg 319, Arg

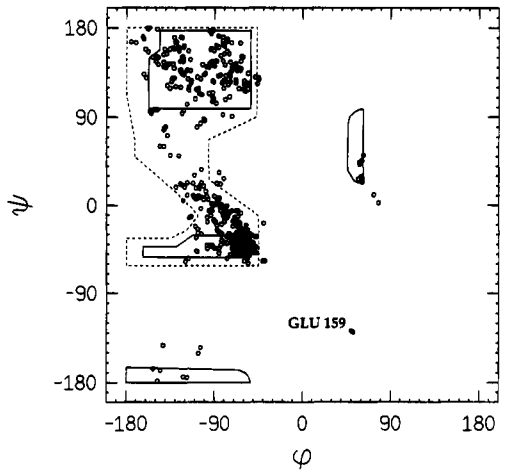

FIGURE 1: Ramachandran plot of all non-glycinyl main-chain dihedral angles for both subunits in the asymmetric unit. Fully allowed ϕ,ψ values are enclosed by solid lines; those partially allowed are enclosed by dashed lines. The only significant outlier is Glu 159 in both subunits. The electron density is unambiguous for this residue, and Glu 159 adopted the same conformation in the apoenzyme structure.

331, Glu 338, Glu 344, and Arg 356 in subunit I and Arg 67, Arg 96, Lys 175, Arg 319, Glu 338, and Glu 344 in subunit II. Phosphotriesterase contains 365 amino acid residues, 29 of which constitute a leader sequence. For both subunits in the asymmetric unit, well-defined electron density was observed starting at Asp 35. The electron density prior to Asp 35 was difficult to interpret although there were several disjointed peaks at 3σ in an electron density map calculated with coefficients of the form $(F_o - F_c)$. In addition, the C-termini for subunits I and II terminated at Arg 363 and Ala 364, respectively. The following discussion will refer to subunit II unless otherwise indicated since it had fewer disordered side chains at the protein surface. It should be noted, however, that the polypeptide chain backbone atoms for the two subunits in the asymmetric unit superimpose with a root-mean-square deviation of 0.15 Å.

RESULTS AND DISCUSSION

The first crystals of phosphotriesterase were grown from 9% poly(ethylene glycol) solutions containing 100 mM bicine and 1 M LiCl at pH 9.0 (Benning *et al.*, 1994). When the structure was subsequently solved, it became clear that the active site metals had been inadvertently removed. While the enzyme was catalytically competent before the crystallization experiments, presumably the high lithium chloride concentration and the use of bicine as the buffer effectively chelated the metals from the enzyme. Consequently, the next step after the apoenzyme structure had been determined was to attempt to reconstitute the enzyme with metal ions in the crystalline lattice. Attempts at such soaking experiments, however, met with limited success. The X-ray diffraction properties of the crystals severely deteriorated upon soaking, for example, in $CdCl_2$ solutions such that it was not possible to collect X-ray data beyond 3.5-Å resolution although the original X-ray data set for the apoenzyme extended beyond 2.0 Å. The next experiment was to attempt crystallization of the holoenzyme from poly(ethylene glycol) in the absence of both lithium chloride and bicine. Again, these crystallization experiments were unsuccessful until the substrate analog, diethyl 4-methylbenzylphosphonate, was added to the precipitant. In the presence of 1% diethyl 4-methylbenzylphosphonate, thin plate-like crystals appeared within 1 week and diffracted to 2.0-Å resolution.

As can be seen in Figure 3a, there are striking structural rearrangements that occur upon binding of the cadmium ions to phosphotriesterase. In retrospect, it is not surprising that the metal-soaking experiments with preformed crystals of the apoenzyme destroyed the crystalline lattice. The root-mean-square deviation between all α-carbon positions for the apo- and holoenzymes is 3.4 Å. These structural

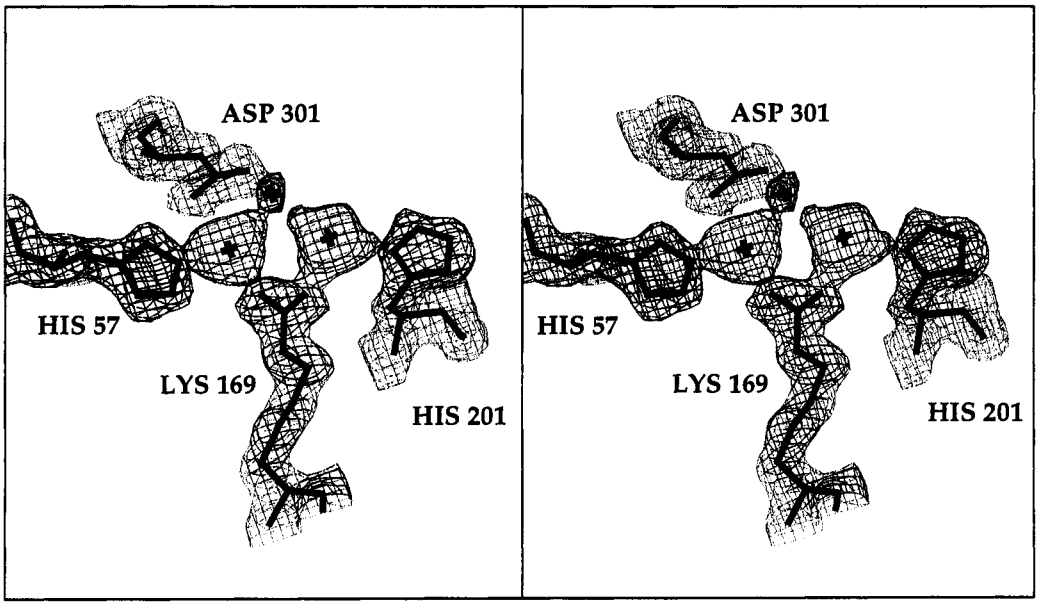

FIGURE 2: Representative portion of the electron density map corresponding to a portion of the binuclear metal center. The electron density displayed was calculated with coefficients of the form $(2F_o - F_c)$ where F_o was the native structure factor amplitude and F_c was the calculated structure factor amplitude from the model refined at 2.0-Å resolution. For the sake of clarity only the electron density corresponding to His 57, His 201, Asp 301, the bridging ligands (Lys 169 and a water molecule), and the two cadmium ions is shown. This figure was prepared with the software package FROST, written by Dr. Gary Wesenberg, and is meant to emphasize the elongated electron density observed for Lys 169 which can be modeled as a carbamate moiety.

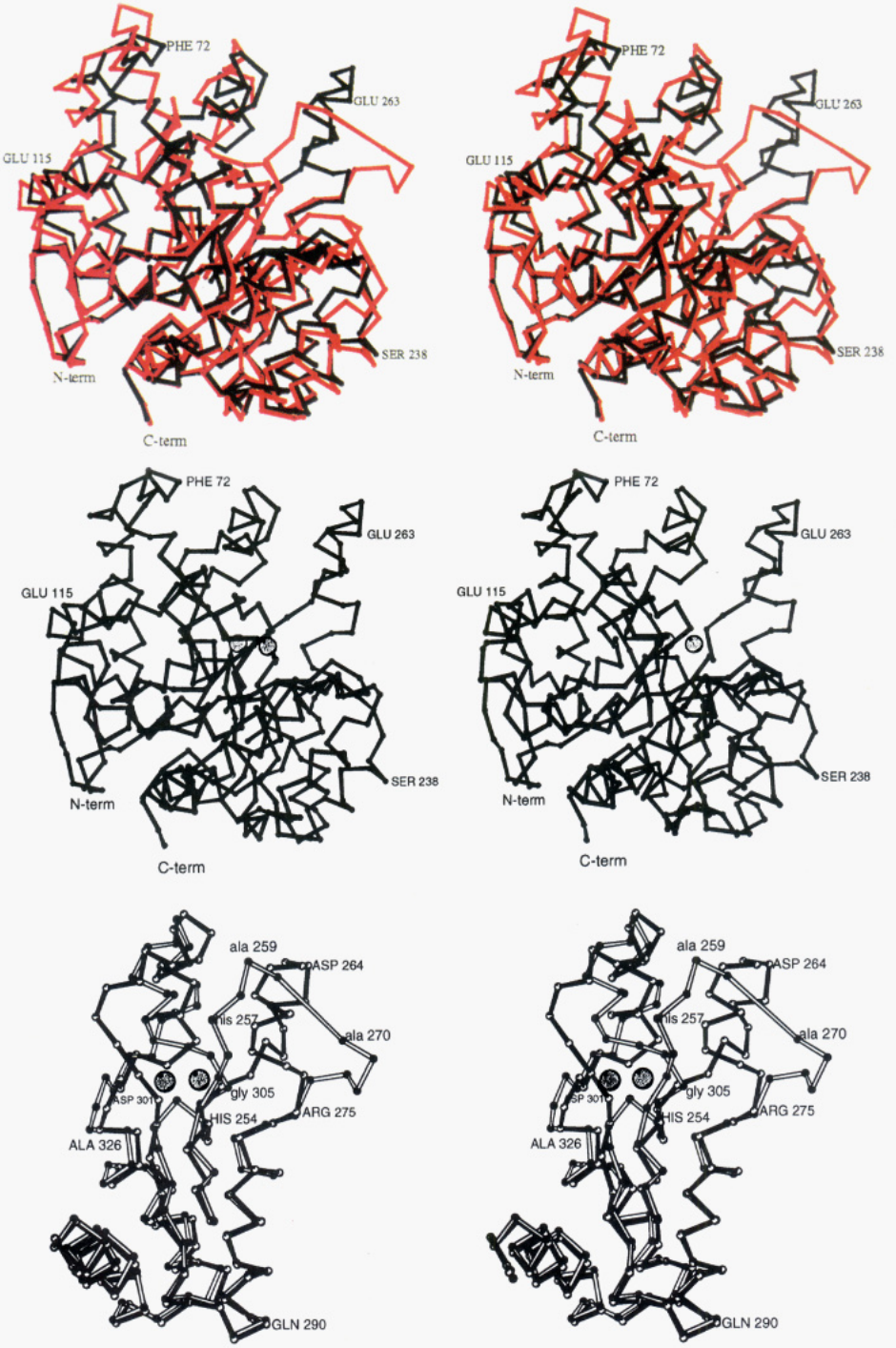

FIGURE 3: Superposition of the α-carbon traces for the apo- and the holoenzyme subunits. This figure was prepared with the plotting package, MOLSCRIPT (Kraulis, 1991). (a, top) The apo and holo forms of the enzyme are shown in red and black, respectively. (b, middle) The holoenzyme alone is shown in the same orientation as in (a) with the positions of the metals depicted in a space-filling representation. (c, bottom) Close-up view of the superposition from Ile 250 to the C-terminus. The apo- and holoenzyme structures are shown in open and closed bonds, respectively. Lower case lettering refers to the apoenzyme while the upper case lettering corresponds to the holoprotein. The cadmium ions are represented as small spheres.

differences, however, are limited to several specific regions such that when removed from the calculation the remaining α-carbon positions for the apo and holo models superimpose with a root-mean-square deviation of 0.65 Å. These regions include Thr 54 to Ala 78, Trp 131 to Leu 136, Val 170 to Gln 180, His 201 to Glu 210, Gly 229 to Tyr 239, Gly 251 to Ser 276, and Val 298 to Pro 322. An α-carbon trace of the holoenzyme with bound metals is given in Figure 3b.

In the apoenzyme there is a type I turn delineated by Gly 60 to Ala 63. In the metal-containing protein this turn has been shifted such that it begins at Ser 62 and ends at Phe 65. These residues adopt a type II rather than a type I turn conformation. In the holoenzyme, there are two type I turns formed by Ala 204 to Arg 207 and His 230 to Asp 233, respectively. These reverse turns are not present in the apoenzyme. One of the most remarkable changes in the holoprotein begins at Leu 252. Here the course of the polypeptide chain changes drastically such that the region delineated by His 254 to His 257 of the holoenzyme superimposes upon the polypeptide chain backbone formed

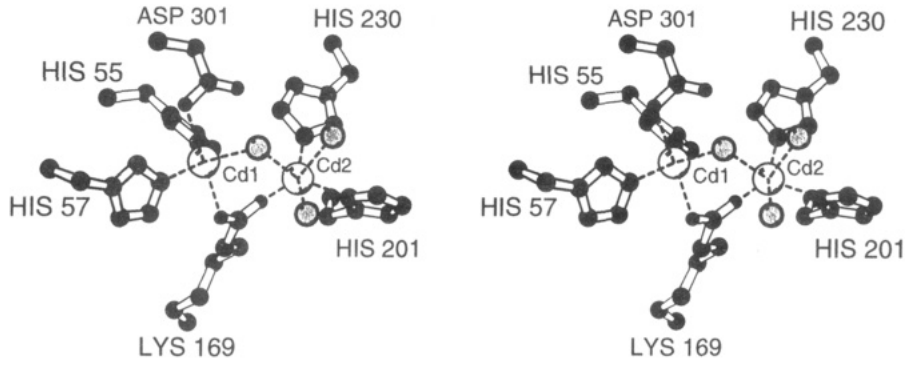

FIGURE 4: Stereoview of the binuclear metal center. The more buried cadmium is located on the left-hand side and adopts a trigonal bipyramidal geometry. The cadmium on the right is ligated by three protein ligands and three solvent molecules in an octahedral arrangement.

by Trp 302 to Gly 305 of the apoprotein as shown in Figure 3c. In the apoprotein, the loop defined by Gly 261 to Ser 269 is disordered whereas in the holoenzyme this region is characterized by a type II turn (Ala 259 to Leu 262), a type I turn (Leu 262 to Asn 265) and an α-helix (Ala 266 to Leu 272). The two proteins begin to superimpose again at Arg 275. The last significant deviation between the two models occurs at Asp 301 where the ϕ,ψ angles for the apo- and holoproteins are −54.2°, −45.2° and 58.3°, 44.0°, respectively. This change from a right-handed to a left-handed helical conformation forces the polypeptide chain into a different direction as can be seen in Figure 3c. The two models again match up at Pro 322. The dramatic differences between the apo- and holoproteins described here highlight the difficulty, especially for metal-containing proteins, in predicting three-dimensional structures based solely on amino acid sequences.

Since the crystals were grown in the presence of diethyl 4-methylbenzylphosphonate, it was anticipated that the active site would contain well-ordered electron density for this substrate analog. Indeed, unambiguous electron density for the inhibitor was located in the map but not in the phosphotriesterase active site. Instead, the inhibitor bound in the interface between two symmetry-related molecules in the crystalline lattice. Specifically the benzyl ring of the substrate analog formed stacking interactions with Phe 51 and Tyr 156. Although disappointing, this compound may have potential use as an additive in future crystallization experiments.

On the basis of site-directed mutagenesis analyses, various models for the phosphotriesterase binuclear metal center have been described recently (Kuo & Raushel, 1994; Lai *et al.*, 1994). Kuo and Raushel have suggested that one metal ion is coordinated to His 55, His 57, His 230, and a water molecule while the other is coordinated to His 254, His 257, a carboxylate group from either an aspartate or a glutamate, and His 230. The investigation of Lai *et al.* (1994) concluded that His 55, His 57, and His 201 ligate one metal and His 254 and His 257 are involved in the second metal ligation sphere.

In light of these site-directed mutagenesis experiments, the phosphotriesterase binuclear metal cluster, as shown in Figure 4, contained several unanticipated features. The first surprise was the presence of a carbamylated lysine as can be seen in the electron density shown in Figure 2. This carbamylated lysine (Lys 169) acts as one of the bridging ligands for the binuclear metal center. It has now been demonstrated that high concentrations of bicarbonate can accelerate the reconstitution of the metals with the apoenzyme and that the reconstitution process can be inhibited by degassing or by the addition of formaldehyde (Hong & Raushel, unpublished results). Most likely, the enzyme employs a carbamylated lysine rather than a glutamate residue because the pair of electrons on the nitrogen can be delocalized, thereby allowing both oxygen ligands to carry negative charges. Carbamylated lysines are not unprecedented and have been observed, for example, in ribulose-1,5-bisphosphate carboxylase where one serves as a ligand to the Mg^{2+} ion (Lorimer *et al.*, 1976). In the apophosphotriesterase model Lys 169 is not carbamylated but rather its ϵ-nitrogen lies in close contact (2.1 Å) to $N^{\epsilon 2}$ of His 201.

Of the six histidine residues clustered at the C-terminus of the β-barrel, four participate directly as ligands to the metals. The more buried of the cadmiums adopts a trigonal bipyramidal geometry with four of the ligands contributed by the protein (His 55, His 57, Lys 169, and Asp 301) and the fifth by a solvent molecule. The axial ligands are formed by the side-chain oxygens from the carbamylated Lys 169 and from Asp 301. Lys 169 and the water molecule act as bridges to the second cadmium. The more solvent exposed metal is surrounded by His 201, His 230, Lys 169, two additional waters, and the bridging water in a distorted octahedral geometry. His 230 forms a stacking interaction with His 254, which in turn participates in a similar interaction with His 257.

A cartoon of the binuclear metal center with appropriate distances is given in Figure 5. The cadmium ions are separated by 3.8 Å. Some caution is necessary in interpreting the positions of the putative water molecules, however. As can be seen in Figure 5, most of the metal−ligand distances between the cadmiums and the waters are longer than would be expected. There is a "tube" of electron density attached to the metal-bridging water that has been difficult to interpret. Presently it has been modeled as two additional water molecules. It is possible, however, that contaminants from either the poly(ethylene glycol) or substrate analog solutions employed for crystallization have bound in the active site pocket at low occupancy. If, indeed, a contaminant has bound in the active site, then the structure of the enzyme presented here may not be that of the resting state. It is conceivable that in the ground state the metals are tetrahedrally coordinated as has been observed for cadmium and zinc ions in proteins. Attempts to grow crystals from recrystallized poly(ethylene glycol) solutions are presently in progress. Also note that the structure described here is of the cadmium-substituted enzyme. Although this enzyme

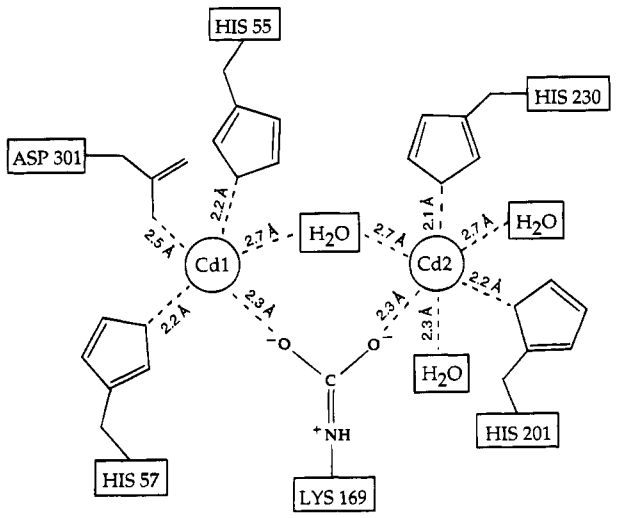

FIGURE 5: Cartoon of the binuclear metal center. The distances quoted are the average values observed for the two subunits in the asymmetric unit.

is catalytically competent, the naturally occurring protein contains 2 mol equiv of zinc. Thus far, it has not been possible to produce crystals of the zinc-containing phosphotriesterase, again suggesting that the local environment around the binuclear metal center may change depending upon the state of the enzyme.

It has been shown that the reaction mechanism of phosphotriesterase proceeds with inversion of configuration about the phosphorus of the substrate (Lewis *et al.*, 1988). The current hypothesis is that the reaction occurs via an S_N2 mechanism whereby an active site base of the protein abstracts a proton from a water molecule. This activated solvent then directly attacks the electrophilic phosphorus of the substrate (Lewis *et al.*, 1988). The only possible active site base within 5.0 Å of the binuclear metal center that is not directly involved in metal chelation is His 254. The other histidine residue, namely, His 257, is over 7 Å from the metal cluster. On the basis of the structural data presented here, an alternative mechanism can be proposed which excludes the necessity for an active site base contributed by an amino acid side chain. It is possible that the bridging solvent molecule, which already may be in the activated form of a hydroxide, acts as the nucleophile. If the phosphoryl oxygen of the substrate binds to the less buried cadmium ion and displaces the bridging hydroxide from the first metal to the second, then both the nucleophile and the substrate would be in the proper position for a single in-line displacement attack. Experiments designed to test this model, including X-ray crystallographic studies of various types of substrate analogs, are in progress.

Phosphotriesterase is unique among the organophosphate-degrading enzymes studied to date in that it is capable of hydrolyzing both widely employed pesticides and the phosphofluoridates, such as sarin and soman, stockpiled by various countries as "chemical warfare deterrents". As a result the enzyme has received considerable attention in recent years. By the combination of X-ray crystallographic studies and site-directed mutagenesis experiments presently underway, it will be possible to more fully explore the enzymatic mechanism of this enzyme. The structure described here represents the initial structural framework for understanding this potentially important bioremediation agent.

ACKNOWLEDGMENT

We thank Drs. W. W. Cleland, I. Rayment, and L. Pedersen for thoughtful advice. The discussions of K. M. Rayment are also gratefully acknowledged.

REFERENCES

Benning, M. M., Kuo, J. M., Raushel, F. M., & Holden, H. M. (1994) *Biochemistry 33*, 15001−15007.
Bernstein, F. C., Koetzle, T. F., Williams, G. J. B., Meyer, E. F., Jr., Brice, M. D., Rogers, J. R., Kennard, O., Shimanouchi, T., & Tasumi, M. (1977) *J. Mol. Biol. 112*, 535−542.
Bricogne, G. (1976) *Acta Crystallogr. A32*, 832−837.
Chae, M. Y., Omburo, G. A., Lindahl, P. A., & Raushel, F. M. (1993) *J. Am. Chem. Soc. 115*, 12173−12174.
Kabsch, W. (1988a) *J. Appl. Crystallogr. 21*, 67−71.
Kabsch, W. (1988b) *J. Appl. Crystallogr. 21*, 916−924.
Kraulis, P. J. (1991) *J. Appl. Crystallogr. 24*, 946−950.
Kuo, J. M., & Raushel, F. M. (1994) *Biochemistry 33*, 4265−4272.
Lai, K., Dave, K. I., & Wild, J. R. (1994) *J. Biol. Chem. 269*, 16579−16584.
Lewis, V. E., Donarski, W. J., Wild, J. R., & Raushel, F. M. (1988) *Biochemistry 27*, 1591−1597.
Lorimer, G. H., Badger, M. R., & Andrews, T. J. (1976) *Biochemistry 15*, 529−536.
Navaza, J. (1987) *Acta Crystallogr. A43*, 645−653.
Omburo, G. A., Kuo, J. M., Mullins, L. S., & Raushel, F. M. (1992) *J. Biol. Chem. 267*, 13278−13283.
Omburo, G. A., Mullins, L. S., & Raushel, F. M. (1993) *Biochemistry 32*, 9148−9155.
Scanlan, T. S., & Reid, R. C. (1995) *Chem. Biol. 2*, 71−75.
Tronrud, D. E., Ten Eyck, L F., & Matthews, B. W. (1987) *Acta Crystallogr. A43*, 489−501.

BI950657A